Monitoring Committee Progress Report #3

Numerical Representation of Mountains in Atmospheric Models

James Shaw

Supervisors: Hilary Weller, John Methven, Terry Davies

Monitoring Committee: Paul Williams, Maarten Ambaum

31st May 2016

1 Introduction

Next-generation atmospheric models are designed to be more flexible than previous models, so that the choice of mesh and choices of numerical schemes can be deferred or changed during operation (Ford et al., 2013; Theurich et al., 2015). My PhD project seeks to make numerical weather and climate predictions more accurate by developing new meshes and numerical schemes that are suitable for next-generation models. In particular, the project addresses the modelling of orographic flows on arbitrary meshes, focusing on three aspects: first, how orography is best represented by a mesh; second, how to accurately advect quantities over orography and, third, how to avoid unphysical solutions in the vertical balance between pressure and temperature.

Representing orography with meshes

There are two main types of mesh used in atmospheric models: terrain-following meshes and cut cells meshes. Terrain-following meshes reduce numerical accuracy in the calculation of horizontal pressure gradients (Gary, 1973; Zängl, 2012) and advection terms (Schär et al., 2002). Inaccuracies are larger near steep terrain. Cut cell meshes are an alternative to terrain-following meshes. Cut cell meshes are orthogonal everywhere except at the surface so that pressure gradient errors and advection errors are reduced, especially near steep terrain (Lock et al., 2012; Good et al., 2014). However, cut cell meshes can have arbitrarily small cells which impose severe constraints on the timestep for explicit methods or semi-implicit methods (Almgren et al., 1997).

To illustrate the two types of mesh, a wave-shaped mountain with a peak height of 1 km is represented using a basic terrain-following mesh (figure 1a) and a cut cell mesh (figure 1b). Notice that the basic terrain-following mesh is severely distorted over steep surfaces while, on the cut cell mesh, small cells are found near the mountain peak. The development of a new type of mesh, the slanted cell mesh, is discussed in section 2.

Advection on arbitrary meshes

Multidimensional advection schemes are attractive because they are suitable for arbitrary meshes (Dubey et al., 2014) and because they avoid splitting errors associated with dimensionally-split schemes (Leonard et al., 1993). However, existing multidimensional schemes are often computationally expensive because a complete polynomial surface must be constructed (Skamarock and Menchaca, 2010). In contrast, the advection scheme by Weller and Shahrokhi (2014) is a multidimensional scheme that achieves computational efficiency by precomputing most flux calculations using the mesh geometry alone. Section 3 describes some of the modifications being made to improve the stability of this advection scheme.

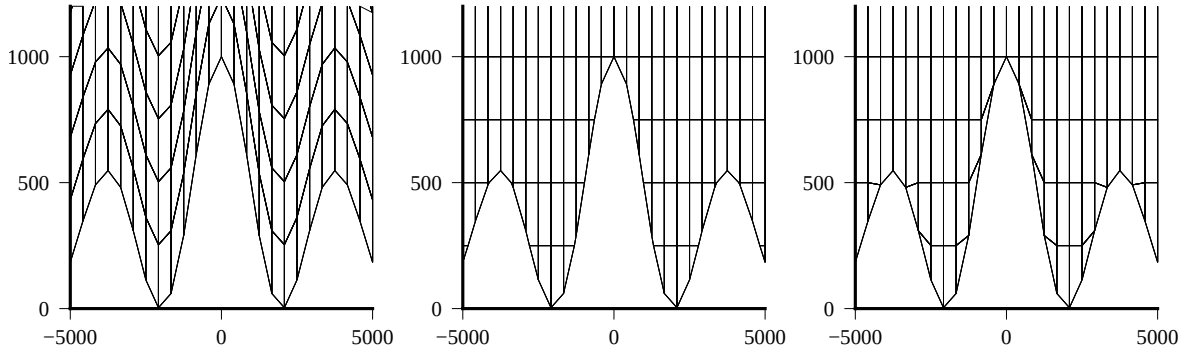

(a) Basic terrain-following mesh (b) Cut cell mesh (c) Slanted cell mesh

Figure 1: Cell edges of basic terrain-following, cut cell and slanted cell meshes having the same wave-shaped mountain profile. Only the lowest 1.2 km in the centre of the domain is shown. The entire domain is 300 km wide and 30 km high. Axis units are m. The cut cell mesh was generated with code used in the All Scale Atmospheric Model (Jähn et al., 2015), kindly provided by the Leibniz Institute for Tropospheric Research.

Vertical balance on arbitrary meshes

Some numerical models are susceptible to computational modes which produce unphysical solutions. Models that have a Lorenz vertical staggering of variables can suffer from one such computational mode (Arakawa and Konor, 1996). The Charney–Phillips vertical staggering does not suffer from the Lorenz computational mode, but it has only been formulated on structured, quadrilateral meshes. I intend to develop a generalisation of the Charney–Phillips staggering for arbitrary meshes, and the necessary tasks are outlined in section 4.

2 Comparison of terrain-following and slanted cell meshes

During the first year of my PhD, I compared the numerical accuracy on terrain-following and slanted cell meshes. In the second monitoring committee report (called MC2 hereafter), a slanted cell mesh was referred to as a cut cell mesh, but it is necessary to make a distinction between the two types: the differences can be seen by comparing the representation of the same terrain profile using cut cells (figure 1b) and slanted cells (figure 1c).

The slanted cell method has advantages over the cut cell method. Shaw and Weller (2016) was published in May 2016 and included the development of a new slanted cell mesh generation method which avoided the complex heuristics employed by the previous method (see MC2, section 3). This method makes slanted cell meshes straightforward to construct, unlike the construction of cut cell meshes, which can be somewhat involved (Hartkopf, 2011). Another advantage of slanted cell meshes is that they alleviate the severe timestep constraints associated with cut cell meshes (Shaw and Weller, 2016).

3 Improving advection on slanted cell meshes

My current work focuses on improving the stability of a multidimensional advection scheme that is suitable for arbitrary meshes (Weller and Shahrokhi, 2014). The performance of the advection scheme is being evaluated over steep slopes on terrain-following, cut cell and slanted cell meshes.

The multidimensional advection scheme is an explicit, Eulerian, method-of-lines, finite-volume scheme that has a cubic upwind-biased stencil. Fluxes across faces are approximated using a least squares polynomial fit onto the stencil point values. On a two-dimensional quadrilateral mesh, the stencil has 4×3 points in the domain interior (figure 2a), but may include fewer points near the boundaries. This is a

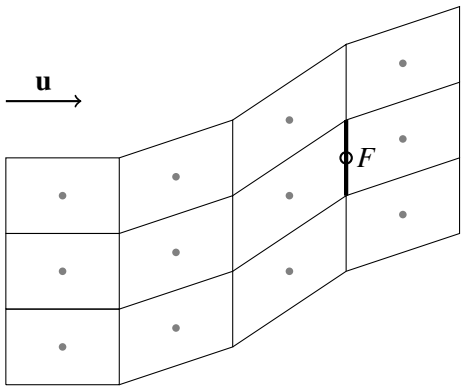

(a) 12-point stencil in the domain interior

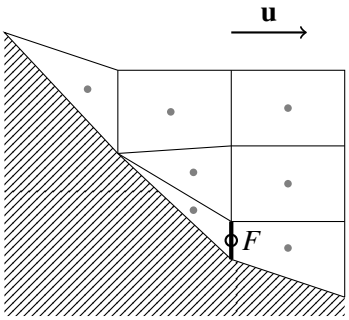

(b) 7-point stencil near the lower boundary of a slanted cell mesh. The ground is shown with diagonal hatching.

Figure 2: Two-dimensional stencils used for approximating a value at a face centroid given a set of surrounding cell centre values. In the two stencils, the face F is shown with a thick line, and the face centroid with an open circle. Cell centres are denoted by grey filled circles. The direction of the wind vector, $\boldsymbol{u}$, is shown above both stencils.

particular concern at the lower boundary where stencils may be smaller and highly distorted (figure 2b).

In the interior of a two-dimensional domain, we fit a polynomial surface to a stencil of a discrete scalar field ϕ:

$$\phi = a_1 + a_2 x + a_3 y + a_4 x^2 + a_5 xy + a_6 y^2 + a_7 x^3 + a_8 x^2 y + a_9 xy^2 \tag{1}$$

where $\boldsymbol{a} = a_1 \ldots a_9$ are the unknown coefficients that are calculated from the least squares fit. It may not be possible to fit all the polynomial terms to a stencil near the lower boundary because it includes fewer points. With additional help from Philip Browne, I have developed a mathematical technique that removes certain high-order terms based on the stencil geometry. We call this technique an 'adaptive polynomial fit'.

The adaptive polynomial fit uses the stencil geometry to construct a full-rank matrix. For a stencil in the interior of a two-dimensional domain with twelve points, $c_1 \ldots c_{12}$, the matrix B is

$$B = \begin{array}{c} \\ c_1 \\ c_2 \\ \vdots \\ c_{12} \end{array} \begin{array}{c} \begin{array}{cccccccccc} \text{constant} & x & y & x^2 & xy & y^2 & x^3 & x^2y & xy^2 & \end{array} \\ \begin{bmatrix} 1 & x_1 & y_1 & x_1^2 & \cdots & \cdots & \cdots & \cdots & x_1 y_1^2 \\ 1 & x_2 & y_2 & x_2^2 & \cdots & \cdots & \cdots & \cdots & x_2 y_2^2 \\ \vdots & \vdots & \vdots & \vdots & & & & & \vdots \\ 1 & x_{12} & y_{12} & x_{12}^2 & \cdots & \cdots & \cdots & \cdots & x_{12} y_{12}^2 \end{bmatrix} \end{array}. \tag{2}$$

Equation (1) is used to form a matrix equation $\boldsymbol{\phi} = B\boldsymbol{a}$, where $\boldsymbol{\phi}$ is the vector of stencil point values that can change between timesteps. To solve for $\boldsymbol{a}$, the pseudo-inverse, $B^\dagger$, is calculated using the singular value decomposition of B. Note that $B^\dagger$ can be precomputed using the stencil geometry alone.

For smaller stencils, or highly-distorted stencil geometries, the matrix B may be numerically rank-deficient (that is, it has singular values close to zero). To ensure that the matrix is full-rank, B is constructed by appending one column at a time. If any column causes the matrix to become rank-deficient then that column is omitted. This technique constructs polynomial surfaces that are high-order for large, uniform stencils and lower-order for smaller stencils or highly-distorted stencils.

The adaptive polynomial fit alone is not enough to ensure numerical stability. I am developing a new procedure that will stabilise the polynomial fit for troublesome stencils. It is based on constraints derived from a one-dimensional von Neumann analysis of a simplified version of the spatial discretisation.

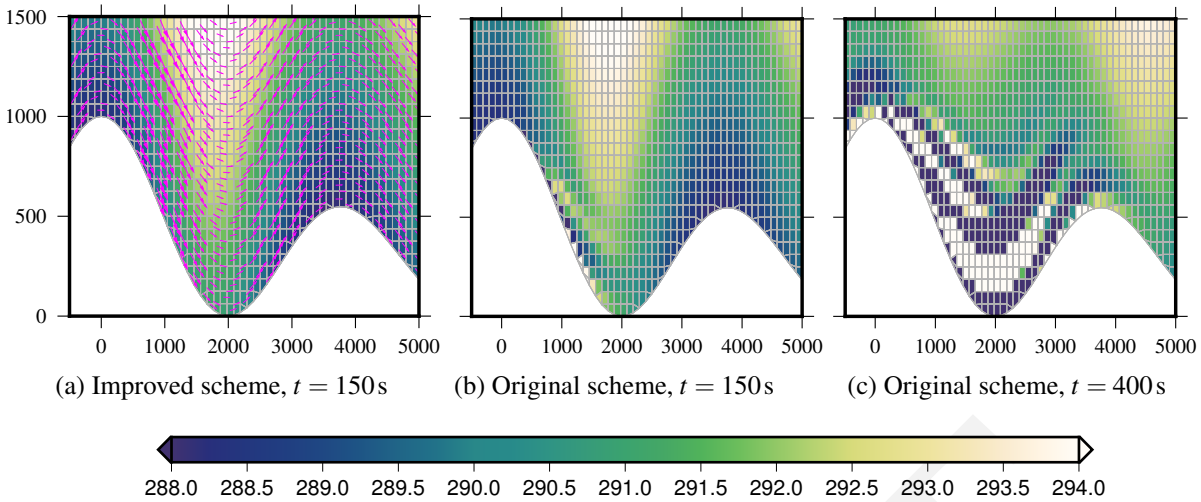

(a) Improved scheme, $t = 150\,\mathrm{s}$ (b) Original scheme, $t = 150\,\mathrm{s}$ (c) Original scheme, $t = 400\,\mathrm{s}$

Figure 3: Comparison of results between the original advection scheme from Weller and Shahrokhi (2014) and the improved advection scheme that includes the adaptive polynomial fit and stabilisation procedures. After $t = 150\,\mathrm{s}$ the initial, stably-stratified thermal profile has been advected in a prescribed, terrain-following wind field over the wave-shaped mountains. The new version of the scheme produces the expected result (subfigure a). With the original version of the scheme, errors develop on the lee slope that are advected along the ground (subfigure b). By $t = 400\,\mathrm{s}$, the instability is fully-developed, having stripes of error and grid-scale oscillations that propagate in a direction opposite to the wind (subfigure c). The timestep is 2.5 s. Cell edges are shown by grey lines. Wind vectors are drawn using magenta arrows, with the wind speed ranging from about $10\,\mathrm{m\,s^{-1}}$ to $13\,\mathrm{m\,s^{-1}}$. The wind field is the same for all results shown and the wind is time invariant. Only the lowest 1.5 km of the central domain is shown. The entire domain is 20 km wide and 5 km. Prior to the construction of the slanted cells, the initially rectangular domain has 192×80 cells. Axis units are m.

Compared to the original version of the advection scheme by Weller and Shahrokhi (2014), the improved version is stable for a wider range of test cases (figure 3). However, the scheme is still weakly unstable in certain cases and work is ongoing to give us confidence that the scheme will be stable and accurate for arbitrary meshes. I am also working with Tristan Pryer here at Reading, and I am reaching out to other experts in the field for suggested solutions.

4 Future research

A timeline of future work is presented with tentative completion dates for each group of tasks. My future work begins with the completion of advection scheme development described in the previous section. After that, I will resume my work developing advection schemes for generalised Charney–Phillips staggering on arbitrary meshes. MC2 discussed a brief exploration into this topic, but no further work has been done since then.

Autumn 2016 Complete stabilisation of the multidimensional advection scheme. We will submit a paper on the topic, noting that the advection scheme is computationally cheap and suitable for arbitrary meshes. Advection tests will be performed over steep slopes and the advantages of the slanted cell mesh will be highlighted.

Spring 2017 Develop a generalised Charney–Phillips staggering for arbitrary meshes. This work comprises a series of tasks:

1. Define the prognostic variables and their arrangement on arbitrary meshes
2. Design a simple numerical scheme for advecting potential temperature

3. Incorporate the advection scheme into the fully-compressible model from Weller and Shahrokhi (2014), using a fully-explicit configuration
4. Compare the Lorenz and Charney–Phillips variants of the model by selecting test that excite the Lorenz computational model, such as the standing waves tests from Arakawa and Konor (1996)

Following this, further tasks should be undertaken if time permits:

5. Adapt the multidimensional cubic advection scheme for advecting potential temperature on generalised Charney–Phillips meshes
6. Modify the fully-compressible model to enable a semi-implicit configuration with the Charney–Phillips staggering

Summer 2017 Write a thesis chapter documenting the generalised Charney–Phillips staggering, the advection scheme and associated work.

Winter 2017 Prepare the thesis introduction and incorporate my other papers into the thesis.

Early 2018 Complete PhD.

5 Personal development

This section discusses some recent activities; a complete training record is provided in the appendix. This year, I have attended almost all lunchtime and departmental seminars, HHH and mesoscale group meetings. I take note of analytical techniques that might be useful in future, for example, verifying trends using low pass filters[1], and solving linear PDEs using Green's functions[2]. I have also peer reviewed a Monthly Weather Review manuscript, and I am keen to get better at critically analysing papers.

Following a talk by Ed Hawkins and Tom Sizmur about online scientific communication, I have been sharing more of my thoughts on my blog and on Twitter[3]. I have found Twitter to be especially useful for discovering contacts from a range of disciplines whose interests overlap with my research.

References

Almgren, A. S., J. B. Bell, P. Colella, and T. Marthaler, 1997: A Cartesian grid projection method for the incompressible Euler equations in complex geometries. **18**, 1289–1309, doi:10.1137/S1064827594273730.

Arakawa, A., and C. S. Konor, 1996: Vertical differencing of the primitive equations based on the Charney-Phillips grid in hybrid σ–p vertical coordinates. *Mon. Wea. Rev.*, **124**, 511–528, doi:10.1175/1520-0493(1996)124<0511:VDOTPE>2.0.CO;2.

Dubey, S., R. Mittal, and P. H. Lauritzen, 2014: A flux-form conservative semi-Lagrangian multitracer transport scheme (FF-CSLAM) for icosahedral-hexagonal grids. *Journal of Advances in Modeling Earth Systems*, **6**, 332–356, doi:10.1002/2013MS000259.

Ford, R., M. Glover, D. Ham, C. Maynard, S. Pickles, and G. Riley, 2013: GungHo phase 1 computational science recommendations. Tech. Rep. 587, UK Met Office. Available at http://www.metoffice.gov.uk/media/pdf/8/o/FRTR587Tagged.pdf.

[1] The summer NAO in observations and CMIP models: impacts on European precipitation and uncertainties in future projected trends, Ileana Bladé, 7 March 2016

[2] Constraining ocean ventilation pathways and time scales with observations and models, Samar Khatiwala, 21 March 2016

[3] My blog is at `datumedge.co.uk` and my Twitter username is @hertzsprrrung

Gary, J. M., 1973: Estimate of truncation error in transformed coordinate, primitive equation atmospheric models. *J. Atmos. Sci.*, **30**, 223–233, doi:10.1175/1520-0469(1973)030<0223:EOTEIT>2.0.CO;2.

Good, B., A. Gadian, S.-J. Lock, and A. Ross, 2014: Performance of the cut-cell method of representing orography in idealized simulations. *Atmos. Sci. Lett.*, **15**, 44–49, doi:10.1002/asl2.465.

Hartkopf, A. M., 2011: MPFA on polyhedral grids in atmospherical applications. Ph.D. thesis, Martin Luther University of Halle-Wittenberg, available at http://asam.tropos.de/wp-content/uploads/diplomarbeit.pdf.

Jähn, M., O. Knoth, M. König, and U. Vogelsberg, 2015: ASAM v2.7: a compressible atmospheric model with a Cartesian cut cell approach. *Geosci. Model Dev.*, **8**, 317–340, doi:10.5194/gmd-8-317-2015.

Leonard, B., M. K. MacVean, and A. P. Lock, 1993: Positivity-preserving numerical schemes for multidimensional advection. Tech. Rep. 106055, NASA Lewis Research Center. Available at http://ntrs.nasa.gov/search.jsp?R=19930017902.

Lock, S.-J., H.-W. Bitzer, A. Coals, A. Gadian, and S. Mobbs, 2012: Demonstration of a cut-cell representation of 3d orography for studies of atmospheric flows over very steep hills. *Mon. Wea. Rev.*, **140**, 411–424, doi:10.1175/MWR-D-11-00069.1.

Schär, C., D. Leuenberger, O. Fuhrer, D. Lüthi, and C. Girard, 2002: A new terrain-following vertical coordinate formulation for atmospheric prediction models. *Mon. Wea. Rev.*, **130**, 2459–2480, doi:10.1175/1520-0493(2002)130<2459:ANTFVC>2.0.CO;2.

Shaw, J., and H. Weller, 2016: Comparison of terrain following and cut cell grids using a non-hydrostatic model. *Mon. Wea. Rev.*, **144**, 2085–2099, doi:10.1175/MWR-D-15-0226.1.

Skamarock, W. C., and M. Menchaca, 2010: Conservative transport schemes for spherical geodesic grids: High-order reconstructions for forward-in-time schemes. *Mon. Wea. Rev.*, **138**, 4497–4508, doi:10.1175/2010MWR3390.1.

Theurich, G., and Coauthors, 2015: The earth system prediction suite: Toward a coordinated U.S. modeling capability. *Bull. Amer. Meteor. Soc.*, doi:10.1175/BAMS-D-14-00164.1, in press.

Weller, H., and A. Shahrokhi, 2014: Curl free pressure gradients over orography in a solution of the fully compressible Euler equations with implicit treatment of acoustic and gravity waves. *Mon. Wea. Rev.*, **142**, 4439–4457, doi:10.1175/MWR-D-14-00054.1.

Zängl, G., 2012: Extending the numerical stability limit of terrain-following coordinate models over steep slopes. *Mon. Wea. Rev.*, **140**, 3722–3733, doi:10.1175/MWR-D-12-00049.1.

Appendix

Mathematics modules

Spring 2016	MA3NAT	Numerical Analysis II	unassessed
Spring 2015	MAMNSP	Numerical Solution of Partial Differential Equations	78%

RRDP modules

24 Mar 2016	Voice coaching: looking after your voice
26–27 Jan 2016	Preparing to teach (introduction, marking & feedback, leading small groups)
2 Dec 2015	An essential guide to critical academic writing
17 Nov 2015	Understanding the UK higher education context
19 May 2015	How to avoid plagiarism
10 Mar 2015	How to write a literature review
19 Feb 2015	How to write a paper

External courses

June 2016	Dynamical core intercomparison project summer school, NCAR
13 May 2016	Peer review: the nuts and bolts, Sense about Science
June 2015	Advanced numerical methods for Earth-system modelling, ECMWF

Conferences and workshops

October 2016	Speaker	Numerical and computational methods for simulation of all-scale geophysical flows, ECMWF
July 2016	Attendee	1st GungHo Network meeting, Daresbury Laboratory
November 2015	Attendee	GungHo workshop on next generation weather and climate prediction, UK Met Office
June 2015	Attendee	Hoskins@70
June 2015	Poster	SCENARIO DTP conference
March 2015	Speaker	Galerkin methods with applications in weather and climate forecasting, ICMS

Teaching

Oct 2015	Teaching assistant	MTMG02 atmospheric physics
Sep 2015	Teaching assistant	NCAS summer school
Sep 2014	Course teacher	MPE python and linux short course

Visits and collaborations

July 2016	Organising visit from Simon Clark, stratospheric PhD researcher and YouTube vlogger
June 2016 –	Working with Hilary's new MSc student, Christiana Skea, studying variable timestepping for ODEs
June 2016	Visiting NCAR, hosted by Ram Nair
2015 – 2016	Coauthoring an article about dimensionally-split and multidimensional advection schemes, written with Hilary, her former student Yumeng Chen, and Stephen Pring at the UK Met Office

Outreach

14 Jul 2015	Schools physicist of the year awards
14 Jun 2015	East Reading festival
15 Feb 2015	Brighton science festival

Presentations

23 Mar 2016	Quo Vadis	Numerical representation of orography in dynamical cores (honourable mention)
17 Feb 2016	PhD group	Multidimensional advection schemes for arbitrary meshes
9 Feb 2016	Mesoscale group	Curl-free pressure gradients for accurate modelling of cold air pools
19 Oct 2015	HHH group	Improving modelled mountain flows with alternative representations of terrain
27 Apr 2015	HHH group	A like-for-like comparison between terrain following and cut cell grids
21 Apr 2015	PhD group	Discrete vector calculus on Arakawa C grids
12 Feb 2015	UK Met Office	Poster presentation for Met Office Academic Partnership
18 Jan 2015	PhD group	Python and linux tips
17 Dec 2014	MPECDT jamboree	Poster presentation for Mathematics for Planet Earth Centre for Doctoral Training jamboree
12 Sep 2014	Lunchtime seminar	Gain control of your documents and code: hands-on with revision control and build automation